Published 2005

# 22 Estimating Tracer Emissions with a Backward Lagrangian Stochastic Technique

**THOMAS K. FLESCH AND JOHN D. WILSON**
*University of Alberta*
*Edmonton, Canada*

Common micrometeorological techniques for determining surface emissions (e.g., eddy covariance, flux gradient, integrated horizontal flux) have two important limitations. On a practical level they require substantial or complex instrumentation: e.g., multiple height measurements of concentration and windspeed, fast-response concentration sensors, etc. A more fundamental problem is the restrictions these techniques place on a measurement site. Most require a flat and homogeneous location with a spatially extensive and uniform source. In many situations these limitations are a problem. The difficulty may be the expense of field equipment, the inconvenience of placing sensors in an appropriate location, or the inability to meet site requirements. One solution might be to use surface chambers, although this technique has other weaknesses and limitations. Another alternative is a method based on a dispersion model.

An atmospheric dispersion model predicts the time-average tracer concentration downwind of a source. By combining this prediction with a field measurement of concentration, one can diagnose a source emission rate. This approach is often called "inverse modeling," since the goal is to deduce information about the source from known downwind concentration, rather than the more common modeling objective of deducing downwind concentration from a known source. Inverse dispersion modeling has been applied to a broad range of problems: from the small scale (observations at distances <10 m from the source) to the continental scale, from point sources to area sources to volume sources, from continuous emission sources to time varying sources; and from neutrally buoyant tracers to "heavy" pathogen spores (e.g., Wilson et al., 1982; Raupach, 1989; Carter et al., 1993; Seibert, 1999; Aylor & Flesch, 2001).

This chapter looks at one type of application of the inverse-dispersion method: the estimation of tracer emissions from a discrete surface area source, using concentration observations taken near the source (within 1 km). This might include emissions from small soil treatment plots, feedlots, ponds, landfills, industrial grounds, etc. We focus on situations where the terrain is "tolerably" homogeneous, and amenable to a Monin-Obukhov similarity description of the surface winds. The advantages of the inverse-dispersion method for these prob-

 *Micrometeorology in Agricultural Systems*, Agronomy Monograph no. 47.

lems are experimental simplicity, the absence of limitations on the size and shape of the source, and flexibility in the type and location of the concentration measurement used to infer emissions. The accuracy of the method rests on having an accurate atmospheric dispersion model. This chapter describes a promising avenue for application of the inverse-dispersion method, the backward Lagrangian stochastic technique. Three example problems are used to illustrate this technique.

## DISPERSION-MODEL-BASED METHOD

Consider the hypothetical problem in Fig. 22–1. A surface area source is emitting a tracer with a continuous and unknown emission rate $Q$ (kg m$^{-2}$ s$^{-1}$). Let us choose a point $M$ within the tracer plume, where the time-average tracer concentration *above background* ($C$) is measured. One can use an atmospheric dispersion model to simulate the transport of tracer from the source to $M$, and predict the ratio of concentration at $M$ to the source emission rate, $(C/Q)_{sim}$. For now, we ignore the details of this prediction. One can then infer the true emission rate as:

$$Q = \frac{C}{\left(C / Q\right)_{sim}} \qquad [1]$$

This is the basis of the inverse-dispersion method: a field measurement $C$ is combined with the model prediction $(C/Q)_{sim}$ to give $Q$.

If the dispersion model accurately mimics atmospheric transport there are no fundamental restrictions on the size or shape of the source. There also is flexi-

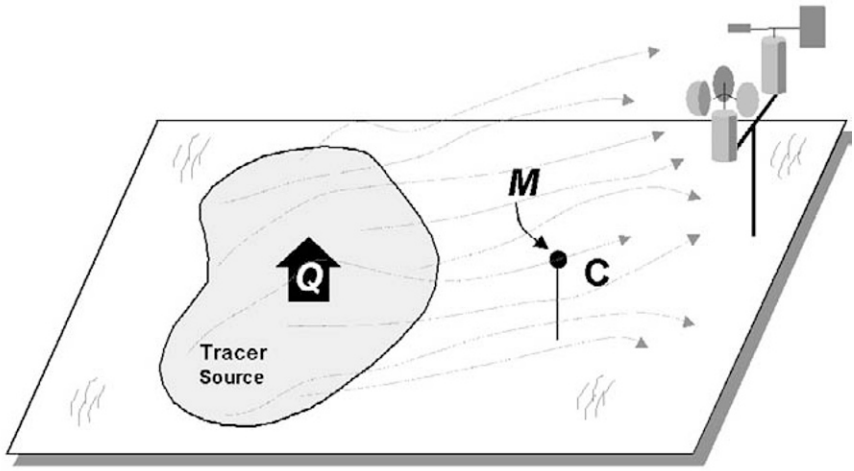


Fig. 22–1. The inverse-dispersion method for estimating tracer emission rate ($Q$). Average tracer concentration $C$ is measured at point $M$. A dispersion model predicts the ratio of concentration at $M$ to the emission rate $(C/Q)_{sim}$.

bility in the location $M$: any point in the emission plume is acceptable in principle. Furthermore, different types of concentration measurements can be used to diagnose $Q$. Any tracer quantity that can be both measured and predicted by a dispersion model (and uniquely related to $Q$) can be employed. For example, a line-average concentration $C_L$ could be substituted for $C$, in which case $(C_L/Q)_{sim}$ would be the object of model prediction. One of the example problems included in this chapter relies on an open-path laser to measure $C_L$.

Equation [1] is deceptively simple, for $(C/Q)_{sim}$ is not a trivial calculation. Many types of dispersion models could provide this prediction (e.g., Gaussian plume, $K$-theory, Lagrangian, etc.). These models have their roots in the scalar mass-conservation equation, where the instantaneous concentration $c$ at time $t$ and position $(x, y, z)$ is given by:

$$\frac{\partial c}{\partial t} + \boldsymbol{u}\frac{\partial c}{\partial x} + \boldsymbol{v}\frac{\partial c}{\partial y} + \boldsymbol{w}\frac{\partial c}{\partial z} = 0 \qquad [2]$$

where $(u, v, w)$ are instantaneous wind velocities in the $x, y, z$ direction (molecular diffusivity and internal tracer source terms are ignored). But Eq. [2] must be time-averaged, transformed, and combined with other information to give $(C/Q)_{sim}$. This operation is difficult and no uniquely correct expression for $(C/Q)_{sim}$ results. Instead there are a variety of solutions, following from a variety of simplifications, giving a variety of dispersion models. These range in complexity from relatively easy-to-use Gaussian plume–puff models (but built on unrealistic assumptions of atmospheric structure) to more rigorous large-eddy simulation models (with a complexity that restricts their use).

Whatever the type of model used to predict $(C/Q)_{sim}$, one must furnish both the average wind and turbulence statistics of the atmosphere. This is a difficult proposition, as wind statistics are spatially and temporally dependent; however, if our interest is short-time intervals in the horizontally homogeneous surface layer (height $z <$ ~100 m, but above a plant canopy), the windflow characteristics are reasonably well-known from a few surface observations. Monin-Obukhov similarity theory (MOST) states that statistical properties of the wind are characterized by the surface drag and buoyancy as quantified by two scaling parameters: the atmospheric friction velocity $u_*$ and the Obukhov stability length $L$ (see Garratt, 1992). A complete wind description also requires the surface roughness length $z_0$ and the wind direction $\beta$. Modeling surface layer dispersion thus requires only specification of $u_*$, $L$, $z_0$, and $\beta$. While their measurement is beyond the scope of this chapter, possible scenarios are:

1. A three-dimensional sonic anemometer is used to: determine $u_*$ from velocity fluctuation covariances; calculate $L$ from the vertical heat flux and $u_*$; and measure $\beta$. The $z_0$ can be inferred from the average wind velocity, $L$, and $u_*$ (i.e., the stability corrected log wind profile can be rearranged to give $z_0$).
2. Windspeed and air temperature are measured at several heights. Fitting these to theoretical wind and temperature profiles yields $u_*$, $z_0$, and $L$. A wind vane gives $\beta$.

3. A single anemometer and qualitative atmospheric observations are used to estimate $L$ (e.g., Pasquill, 1961; Gifford, 1976). The $z_0$ is inferred from the surface cover (bare soil, short grass, etc.). Then $u_*$ is calculated from windspeed, $z_0$, and $L$. A vane gives $\beta$.

An "ideal surface-layer problem" is defined as one needing only a MOST description of the atmosphere to accurately predict $(C/Q)_{sim}$. This would be the case when the emission source and point $M$ lie in the horizontally homogeneous surface layer, where tracer dispersion above the surface layer was inconsequential (e.g., the source-to-$M$ distance < ~1000 m), and dispersion within a plant canopy can be neglected (i.e., $M$ is well above the canopy).

There is no fundamental reason to limit the inverse-dispersion method to ideal surface-layer problems (or surface area sources). Dispersion models have been used successfully over continental scales, within plant canopies, around buildings, behind fences, in forest clearings, etc. The capability to infer $Q$ in these non-ideal settings is an advantage of the method when compared with other techniques; however, such problems require a more complicated treatment of dispersion, and the ability to accurately model dispersion in complicated flows is less certain. Fortunately there are many agricultural and environmental problems that potentially fit under the category of an "ideal surface-layer problem." The rest of this chapter focuses on such cases, and highlights the simplicity of the backward Lagrangian stochastic (bLS) dispersion model as the basis for emission inference in these problems.

## BACKWARD LAGRANGIAN STOCHASTIC TECHNIQUE

The success of the inverse-dispersion method depends upon an accurate dispersion model. To be broadly useful the model also should be easy-to-use, even by non-specialists. The backward Lagrangian stochastic model meets these dual objectives, having the proven accuracy of traditional forward Lagrangian stochastic models but with greater simplicity and flexibility.

### Forward LS Models

The most natural and accurate means of modeling atmospheric dispersion is the Lagrangian stochastic (LS) approach (Wilson & Sawford, 1996). A forward LS model mimics the trajectories of thousands of tracer "particles" as they travel downwind of a source. Each trajectory is made up of a series of discrete changes in particle position and velocity. The changes in position $\Delta x_i$ ($x_1$, $x_2$, $x_3$ = $x$, $y$, $z$: the along-wind, across-wind, and vertical coordinates) and velocity $\Delta u_i$ ($u_1$, $u_2$, $u_3$ = $u$, $v$, $w$: the along-wind, across-wind, and vertical velocities) over a model timestep $\Delta t$ are calculated with Langevin equations:

$$\Delta u_i = a_i \Delta t + b_i R_i,$$
$$\Delta x_i = u_i \Delta t, \qquad [3]$$

where the coefficients $a_i$ and $b_i$ are functions of position and velocity, and $R_i$ is a Gaussian random number (from a population having zero average and variance

$\Delta t$). The model timestep $\Delta t$ is typically of order 0.1 to 10 s (a fraction of the local turbulence timescale).

The correct form of $a_i$ and $b_i$ in the atmosphere is an ongoing research problem—as yet there is no uniquely correct solution for these coefficients in multi-dimensional models; however, the solution given by Thomson (1987) for Gaussian turbulence (i.e., probability density functions for Eulerian velocities are Gaussian) is widely used. This solution requires specification of the time-average Eulerian velocity statistics: the average wind velocity in each component ($U$, $V$, $W$), the variance of the velocity fluctuations ($\sigma_u^2$, $\sigma_v^2$, $\sigma_w^2$), the velocity fluctuation covariances ($\langle u'v' \rangle$, $\langle u'w' \rangle$, $\langle v'w' \rangle$), and the turbulent kinetic energy dissipation rate ($\varepsilon$). In the ideal surface layer we assume the average vertical velocity $W = 0$, and by placement of the $y$ coordinate perpendicular to the average wind direction take $V = \langle u'v' \rangle = \langle v'w' \rangle = 0$, and $\langle u'w' \rangle = -u_*^2$. If we furthermore approximate $u_*$, $\sigma_u^2$, and $\sigma_v^2$ as constant with height (but allow $\sigma w^2$ to be height dependent), Thomson's solution reduces to:

$$a_u(u,v,w,z) = -\frac{b_u^2}{2\left(\sigma_u^2\sigma_w^2 - u_*^4\right)}\left[\sigma_w^2\left(u-U\right) + u_*^2 w\right] + w\frac{\partial U}{\partial z},$$

$$a_v(u,v,w,z) = -\frac{b_v^2}{2\sigma_v^2}v,$$

$$a_w(u,v,w,z) = -\frac{b_w^2}{2\left(\sigma_u^2\sigma_w^2 - u_*^4\right)}\left[u_*^2\left(u-U\right) + \sigma_u^2 w\right] + \frac{1}{2}\frac{\partial \sigma_w^2}{\partial z}$$
$$+\frac{1}{2\left(\sigma_u^2\sigma_w^2 - u_*^4\right)}\left[u_*^2\frac{\partial \sigma_w^2}{\partial z}\left(u-U\right)w + \sigma_u^2\frac{\partial \sigma_w^2}{\partial z}w^2\right]. \qquad [4]$$

The stochastic coefficients are:

$$b_u = b_v = b_w = b = \sqrt{C_0\varepsilon}, \qquad [5]$$

where $C_0$ is a "universal" constant[1]. A more traditional definition is $b = (2\sigma_w^2/T_L)^{1/2}$, where $T_L$ is a Lagrangian timescale (Wilson et al., 1981, give formulae for $T_L$).

The atmospheric statistics needed to implement Thomson's solution ($U$, $\sigma_u^2$, $\sigma_v^2$, $\sigma_w^2$, $\varepsilon$) are reasonably well known for the surface layer if one knows $u_*$, $L$, and $z_0$ (common formulae are given by Panofsky et al., 1977; Hanna, 1982; Rodean, 1996, etc.). With these statistics specified, the calculation of $(C/Q)_{sim}$ for location $M$ is straightforward. Thousands of model particles are released with uniform density across the source area, each being given a random initial velocity consistent with $U$, $\sigma_u^2$, $\sigma_v^2$, $\sigma_w^2$ at the source location. Downwind trajectories are calculated using Eq. [3]. A "sensor volume" is placed around $M$, and the particle residence time in this volume gives $(C/Q)_{sim}$ (see Flesch et al., 1995).

[1]Reported values of $C_0$ range between 2 and 9. Wilson et al. (2001) found $C_0 \approx 4.5$ gave LS model agreement with experimental data (for traditional parameterizations of $\sigma_w$ and $\varepsilon$).

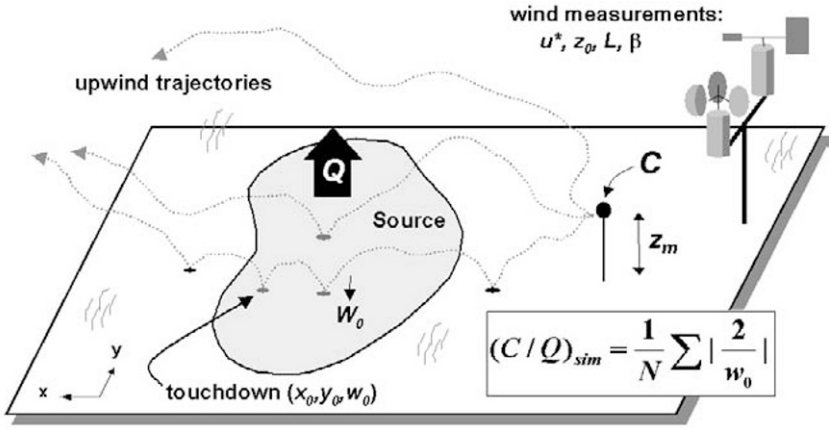


Fig. 22–2. Illustration of the bLS technique for estimating tracer emission rate ($Q$). Average concentration $C$ is measured downwind of the source, with $u_*$, $z_0$, $L$, and β determined from wind measurements. Backward (upwind) trajectories are calculated using a bLS model. The ratio $(C/Q)_{sim}$ is calculated from trajectory "touchdowns" inside the source.

## Backward LS Models

The "backward" LS approach is a particularly efficient way of determining $(C/Q)_{sim}$ for surface area sources (Flesch et al., 1995). In a backward LS model (denoted bLS) the *upwind* trajectories of tracer particles are calculated from point $M$ (Fig. 22–2). Only a slight modification of the above Langevin model is needed to transform the forward model to a backward model: the time increment $\Delta t$ will now be negative, and the negative sign of the first term on the right-hand side of each $a$ coefficient (the "fading memory" terms in Eq. [4]) is reversed.

The important information in an ensemble of backward trajectories originating from $M$ is the location $(x_0, y_0)$ where particles impact the ground ("touchdowns")[2], and the vertical "touchdown velocity" at impact, $w_0$. The calculation of $(C/Q)_{sim}$ focuses on the touchdowns within the source boundary:

$$\left(C / Q\right)_{\text{sim}} = \frac{1}{N}\sum\left|\frac{2}{w_0}\right| \qquad [6]$$

where $N$ is the total number of particles released from $M$, and the summation covers only touchdowns within the source. The summation in Eq. [6] is the equivalent residence time of particles inside the source "volume" (i.e., for an infinitesimally thin source layer), a quantity that corresponds to the average concentration "in" the source. So the concentration at point $M$ due to an area source can be alternatively calculated as the average concentration "within" the area source due to a release of tracer from $M$—using a properly calculated set of back-

[2]LS models do not resolve the atmosphere below a reflection height $z_r$. This height is referred to as the ground, but it may be significantly above ground. When a model particle crosses below $z_r$ (i.e., a touchdown) it is reflected back into the resolved atmosphere.

ward trajectories. Hereafter the term "bLS technique" will refer to the implementation of the inverse-dispersion method with this bLS calculation.

An attraction of the bLS technique is the ease with which complex source shapes can be handled. After creating an ensemble of touchdowns, all that is required is a method of separating those inside and outside the source. Flesch et al. (1995) also found that backward models are generally more efficient than forward models for simulating short-range dispersion from an area source (i.e., fewer model particles needed). A more substantial advantage is the ability to prerun the dispersion model without knowledge of the eventual source geometry (for a horizontally homogeneous atmosphere). An important consequence of a simple MOST parameterization of the wind field (with $U$, $\sigma_u$, $\sigma_v$, $\sigma_w$, and $\varepsilon$ scaled on $u_*$) is that the bLS touchdown field ($x_0$, $y_0$, $w_0/u_*$) has generality:

1. $x_0$ and $y_0$ are independent of windspeed (for given $L$, $z_0$, and release height $z_m$);
2. $x_0$ and $y_0$ can be horizontally translated to different $M$ locations;
3. $x_0$ and $y_0$ can be rotated with changing wind direction;
4. $w_0/u_*$ is independent of windspeed (for given $L$, $z_0$, and $z_m$).

Thus, for a given $z_0$, $L$, and $z_m$, a single touchdown catalog ($x_0$, $y_0$, $w_0/u_*$) provides the solution to any future problem. A set of catalogs can be calculated in advance, and later mapped onto a particular problem geometry, so that $(C/Q)_{sim}$ can be calculated from touchdowns occurring within the source.

## Using a Line-averaging Concentration Sensor

An advantage of the inverse-dispersion method is flexibility in the type of concentration measurement used to deduce $Q$. For instance, an open-path laser can measure line-average tracer concentration ($C_L$) along an atmospheric path. The bLS technique can be modified to predict $(C_L/Q)_{sim}$. For a horizontal path this is done easily, by simulating $C_L$ as the average of many point measurements equispaced along the path, and repeatedly translating the touchdown catalog to these points along the path.

Using a line-averaging sensor has the potential to reduce error in the inverse-dispersion method. Consider a small area source emitting tracer, with a laser positioned downwind of the source and having a long path perpendicular to the wind (completely traversing the plume by a large margin). Here the value of $C_L$ is independent of the lateral spread of the plume: the tracer mass in the path is independent of the $y$ position of the tracer elements. The predicted $(C_L/Q)_{sim}$ will be similarly insensitive to the modeled lateral dispersion, and insensitive to model errors. This is an important consideration, as modeling horizontal dispersion is more error prone than modeling vertical dispersion. This is due to the greater, and less predictable, range of turbulent scales dispersing material in the horizontal. The use of line-average concentration observations can therefore be beneficial for the inverse-dispersion method.

## Potential Errors

The accuracy of the bLS technique in diagnosing an emission rate ($Q_{bLS}$) depends upon: (i) accurate field measurements of concentration; (ii) accurate

meteorological measurements; (iii) an accurate map of the tracer source and sensor; (iv) having no additional tracer sources immediately upwind of the source of interest; and (v) accuracy in the bLS dispersion model. A brief discussion of some of these errors follows.

### Errors in $C$

Errors in the $Q_{bLS}$ are proportional to errors in $C$: a 10% error in $C$ will result in a 10% error in $Q_{bLS}$.

### Errors in $u_*$, $L$, and $z_0$

Errors in these meteorological parameters will result in remove incorrect wind statistics in bLS model. It is difficult to generalize the effect of these errors on $Q_{bLS}$, as this depends on the size and location of the source (some $M$ locations will have very large sensitivity to these errors, while other locations will not).

### Location of Meteorological Observations

Values of $u_*$, $L$, $z_0$, and $\beta$ should be representative of the atmosphere over the site. In horizontally homogeneous terrain the measurement location is not critical. But if the bLS technique is applied to somewhat inhomogeneous situations (but not so seriously non-uniform as to render $Q_{bLS}$ unusable), then there is an evolution of windflow over the terrain, and ambiguity in the proper measurement location (an intuitive choice would be between the tracer source and point $M$). An example of this problem is given in Wilson et al. (2001) for a lagoon source.

### Appropriate Measurement Intervals

Measurement intervals (for $C$, $u_*$, etc.) should be consistent with the internal bLS description of the atmosphere: traditional MOST formulae built from 15 to 60 min average wind statistics. The proper measurement interval should therefore be 15 to 60 min; however, intervals as short as three minutes (Flesch et al., 1995) and as long as 4 h (Flesch et al., 2002) have been used.

### Accurate Problem Map

For most problems an accurate map of the source-sensor layout is crucial, as $(C/Q)_{sim}$ depends on the distance and direction of point $M$ from the source, the source dimensions, and wind direction (the exception is when point $M$ is inside a large source). This demands an accurate problem map. A handheld global positioning system (GPS) unit is an ideal tool for this task.

### No Additional Nearby Tracer Sources

Distant tracer sources, which cause an essentially uniform background concentration $C_b$ over the landscape, are not a problem. Then $C$ is just the average concentration above background. A more difficult problem arises with nearby sources (how near depends on problem geometry). Then there is an intermingling of evolving tracer plumes, which confounds the apportionment of tracer to any

one source. In theory, allocating tracers to multiple sources is possible, but it requires multiple concentration measurements (at different locations) with the potential for very large uncertainties.

### Inaccuracy in the bLS Model

For uniform terrain and typical daytime conditions there is little doubt as to the overall accuracy of LS dispersion models (Wilson & Sawford, 1996); however, there is inherent uncertainty in any dispersion model calculation. Model predictions represent the hypothetical average of many tracer releases, all made under identical conditions. The stochastic variability that exists in any one release is not represented. Therefore it is unrealistic to expect a *one-time* inference of $Q$ to be better than perhaps ±10%, even with perfect knowledge of the wind statistics (similar uncertainties exist in other micrometeorological techniques). And of course there is never perfect knowledge of the wind statistics, so there is additional variability in $Q_{\mathrm{bLS}}$ due to variability in atmospheric statistics about the average represented by the MOST formulae. More significant errors should be expected during periods of extreme atmospheric stratification or rapid atmospheric transitions (e.g., sunrise), given the likely inapplicability of MOST (Garratt, 1992). Model accuracy also will depend on the position of $M$. The bLS model will more accurately predict $(C/Q)_{\mathrm{sim}}$ near the plume centerline than at the plume edge (where plume characteristics are defined by the more extreme, and so less predictable, tracer paths).

## USING THE BLS TECHNIQUE: CASE STUDIES

The following three examples illustrate application of the bLS technique. In the first two examples the emission source is in flat and open terrain, and the vegetation was short or nonexistent. These can readily be classified as "ideal surface-layer problems." The third example takes place in a more complex setting, around a hog-waste lagoon, where care must be taken to ensure an ideal surface-layer environment.

A computer program was designed to simplify application of the bLS technique in these problems. It combines a MOST bLS model (see Flesch et al., 1995) with a GIS-type interface. The user draws the emission source and concentration sensor on a map, and enters $C$ and the atmospheric conditions ($z_0$, $L$, $\beta$). In the present applications the windspeed $S$ at height $z_{\mathrm{m}}$ was used as an input, with $u_*$ calculated internally based on $S$, $z_0$, and $L$. The appropriate touchdown catalog (for the given $L$, $z_0$, and $z_{\mathrm{m}}$) was either created ab initio by running the Lagrangian model or selected from a previously created "library" of catalogs, and then overlaid onto the map. Touchdowns within the source were identified and used to calculate $Q_{\mathrm{bLS}}$.

### Chemical Evaporation from a Small Area Source

Flesch et al. (1995) described an experiment where the bLS technique was used to calculate $Q$ from a small surface source. Volatile chemicals were applied

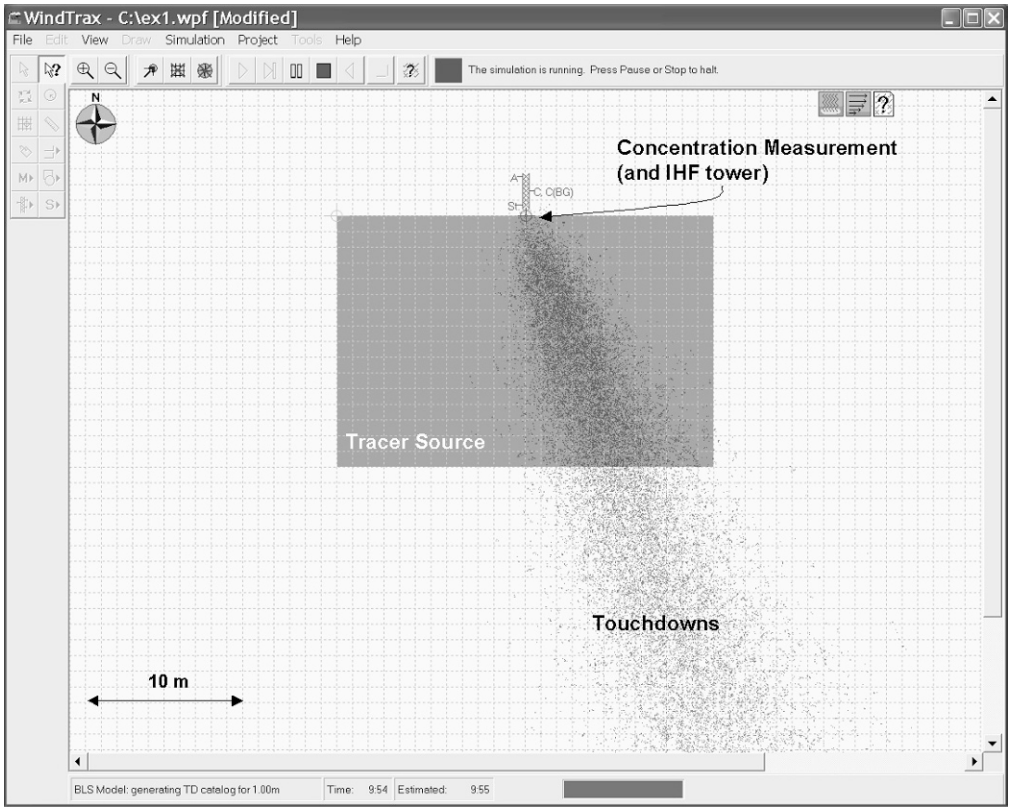


Fig. 22–3. Layout of the chemical evaporation study. Average tracer concentration $C$ was measured at the downwind edge of the source. The small points extending to the lower right of the tower are touchdowns for a southeasterly wind ($\beta = 160°$) and neutral stability.

to create rectangular sources of either 24 × 16 m, 48 × 16 m, or 100 × 25 m. Chemical concentration and winds were measured near the downwind edge of these sources, across intervals from 0–3 to 210–300 min after contamination. The $Q_{bLS}$ predictions were based on windspeed $S$ and concentration $C$ measured at $z_m$ = 1 m. The experiments took place in near-neutral stability over an expansive shortgrass plain ($z_0 \approx 0.025$ m).

The first step was to create a problem map (see Fig. 22–3). Then a touchdown catalog was created, using 15 000 model particles, $z_0 = 0.025$ m, and neutral stability. For each $C$ observation this catalog was rotated to the proper wind direction, overlaid on the problem map, and $Q_{bLS}$ was calculated from touchdowns in the source (Fig. 22–3). Independent estimates of $Q$ were given by integrated horizontal flux (IHF) measurements (see Denmead & Raupach, 1993). Vertical profiles of $C$ and $S$ at the downwind edge of the source gave:

$$Q_{IHF} = \frac{1}{D}\int_{z=0}^{\infty} C(z)S(z)dz, \qquad [7]$$

where $D$ is the along-wind source length. Eq. [7] neglects the turbulent flux of tracer past the sensor array, likely resulting in $Q_{IHF}$ overestimating $Q$ by about 10% (Wilson & Shum, 1992).

Figure 22–4 shows evolution of emissions from one of the experiments. Notice the rapid decrease in emissions as evaporation proceeded. The bLS estimates tracked $Q_{IHF}$ closely. In this example $Q_{bLS}$ was initially smaller than $Q_{IHF}$, but this bias disappeared over time. Perhaps the early bias was due to an inadequate averaging times (as short as three minutes). A comparison of $Q_{bLS}$ and $Q_{IHF}$ over all experiments showed excellent agreement: an overall 2% bias in the $Q_{bLS}$ predictions (although $Q_{IHF}$ overprediction was ignored), with a 15% scatter in individual predictions.

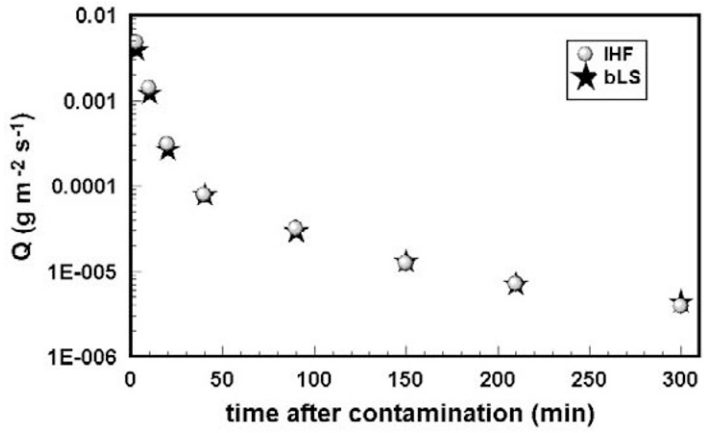


Fig. 22–4. Time evolution of tracer emission rate ($Q$) from one chemical evaporation experiment as estimated by the IHF mass balance technique and the bLS technique.

Table 22–1. Fractional change in bLS estimates of $Q$ ($\delta Q_{bLS}/Q_{bLS}$) to changes in measurement variables for the three example problems presented in this chapter. The additional Case 4 is the lagoon experiment using a different concentration measurement height $z_m$.

| | $\delta Q_{bLS}/Q_{bLS}$ | | | |
|---|---|---|---|---|
| Variable Change | Case 1† | Case 2† | Case 3† | Case 4† |
| $S$ increased 10% | 0.1 | 0.1 | 0.1 | 0.1 |
| $C$ increased 10% | 0.1 | 0.1 | 0.1 | 0.1 |
| $z_0$ increased 50% | –0.03 | 0.06 | –0.1 | –0.07 |
| $z_0$ decreased 50% | 0.18 | –0.07 | 0.18 | 0.13 |
| $L$ = –10 m | 0.13 | 0.45 | –0.24 | –0.09 |
| $L$ = + 10 m | 0.08 | –0.3 | 0.61 | 0.2 |
| Source dimensions increased 10% | –0.09 | –0.05 | –0.22 | –0.2 |
| $C$ moved 1 m downwind | –0.05 | –0.004 | –0.07 | –0.06 |
| $z_m$ increased 10% | 0.13 | 0.06 | 0.21 | 0.04 |
| β increased 10° | –0.02 | –0.01 | –0.08 | –0.07 |

†Case 1, (small rectangular source): $L = \infty$, $\beta = 180°$, $z_m = 1.0$ m, $z_0 = 0.025$ m; Case 2 (large field source): $L = \infty$, $\beta = 180°$, $z_m = 1.05$ m, $z_0 = 0.008$ m; Case 3 (lagoon): $L = \infty$, $\beta = 270°$, $z_m = 1.4$ m, $z_0 = 0.005$ m; Case 4 (lagoon): identical to Case 3, but with $z_m$=1.0 m.

This problem also provides an opportunity to examine the sensitivity of $Q_{bLS}$ to various measurement errors. Table 22–1 lists the fractional change in $Q_{bLS}$ for changes in input variables (for neutral stability and southerly winds)[3]. For example, if $z_0$ is increased 50% while other variables are unchanged, $Q_{bLS}$ decreases 3%. Here the bLS estimates are insensitive to an overestimate of $z_0$. There also is low sensitivity to atmospheric stability, to minor changes in wind direction, to the size of the source, and to the $x$,$y$ position of $C$. Overall this problem is insensitive to measurement errors (at least for a southerly wind), indicating a good measurement location.

The small tracer source in this example shows one major advantage of the bLS technique: the ability to examine sources that are too small to quantify with more common micrometeorological techniques. This study also showed that in an ideal setting (horizontally homogeneous terrain) the bLS technique should predict $Q$ to within approximately 20% for individual one-time estimates, with greater accuracy for multi-observation averages.

## Pesticide Volatilization from a Large Field

Flesch et al. (2002) used the bLS technique to estimate pesticide volatilization (metolachlor) from a bare field after a surface application. Average metolachlor concentration was measured at several heights near the center of the field and used to calculate $Q_{bLS}$. The field was large and located in flat and open terrain in central Iowa.

The site layout, with an example of an overlaid touchdown catalog, is given in Fig. 22–5. Profiles of windspeed $S$ and a sensible heat flux observation gave the meteorological information needed to run the bLS model. Nineteen observation

[3] Some of these results are specific to the particular procedure used to implement the bLS analysis. For example, errors in $z_0$ result in errors in $u_*$ (because $u_*$ is calculated fron $S$, $z_0$, and $L$). A program that takes $u_*$ as an independent input will show different sensitivity to $z_0$.

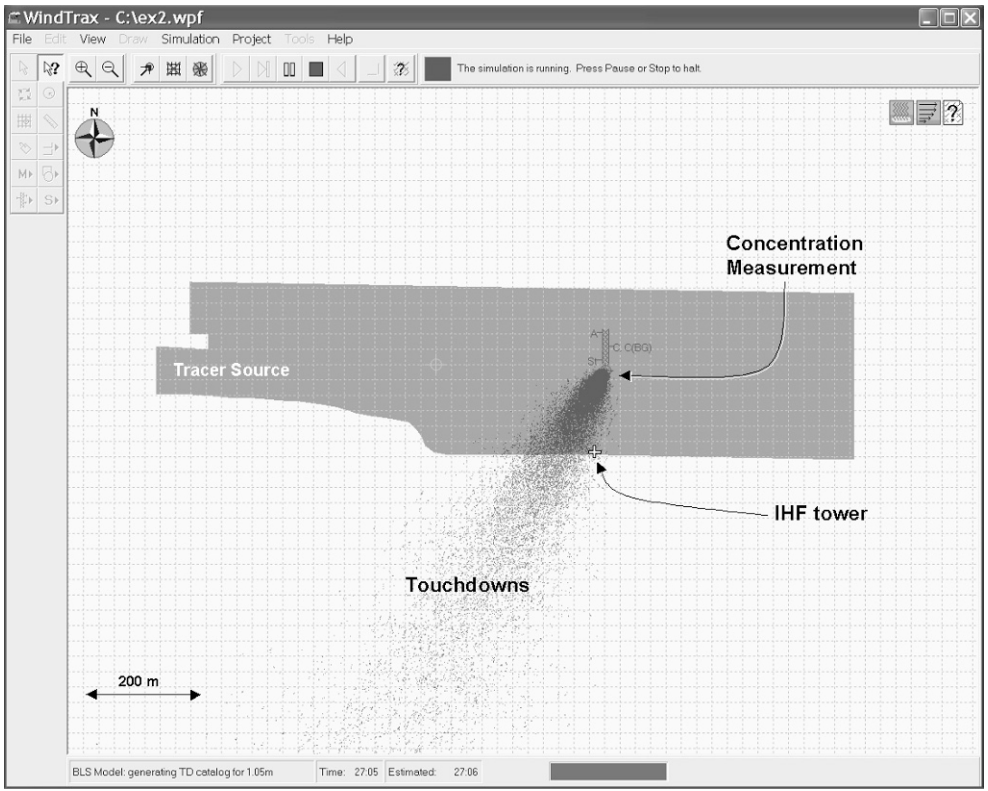


Fig. 22–5. Layout of the pesticide emission study. Average metolachlor concentrations were measured at several heights on a central tower. The small points extending from the tower to the lower left are touchdowns for a measurement height $z_m = 1.05$ m, a southwesterly wind ($\beta = 210°$), and an unstable atmosphere ($L = -10$ m). Emission rates also were measured using the IHF technique near the upwind edge of the field.

periods were used to calculate $Q_{bLS}$, using touchdown catalogs with the appropriate $L$ for each period. It is interesting to compare the example touchdown catalog in Fig. 22–5, which is for unstable atmospheric stratification, with the neutral catalog in Fig. 22–3 (keeping in mind the very different map scales). Greater turbulence in an unstable atmosphere results in a catalog that is broader in the crosswind direction, denser near the sensor (more rapid vertical mixing gives a measurement "footprint" nearer the sensor), and that extends slightly upwind.

Integrated horizontal flux measurements ($Q_{IHF}$) were made near the edge of the field (Eq. [7]) to compare with $Q_{bLS}$; the $Q_{IHF}$ estimates here having been reduced to account for the neglected turbulent flux. The ratio $Q_{bLS}/Q_{IHF}$ averaged 1.06 (Fig. 22–6) indicating an average bLS overprediction of 6%; however, the variability between observations was high, with $Q_{bLS}/Q_{IHF}$ ranging from 0.4 to 1.95. Flesch et al. (2002) attribute some of this variability to measurement uncertainty in $C$. The long measurement intervals used in this experiment (either 2 or 4 h) may also have contributed to large uncertainties: as the sampling interval increases the assumption of atmospheric stationarity becomes less realistic. For instance, if β is changing during an interval the $C$ "footprint" (the ground area from which tracer emissions influence measurement—given by the touchdown map) will be broader than predicted by a bLS simulation that assumes a constant β. The longer the measurement interval, the greater the potential for departure from stationarity, and the greater the likelihood of inaccuracy in the MOST statistics used in the bLS model.

The sensitivity of the bLS estimates to measurement errors in this problem can be deduced from Table 22–1 (for southerly winds, neutral stability, $z_m$ = 1.05 m). For example, if $L$ is changed to –10 m (a strongly unstable atmosphere) while other variables are unchanged, $Q_{bLS}$ increases 45%. We therefore conclude the bLS estimates are sensitive to atmospheric stability errors; however, there is low sensitivity to other errors: $z_0$, source size, $C$ location, and wind direction. This is different from the previous example, where $Q_{bLS}$ was sensitive to $C$ measurement location errors, but not atmospheric stability.

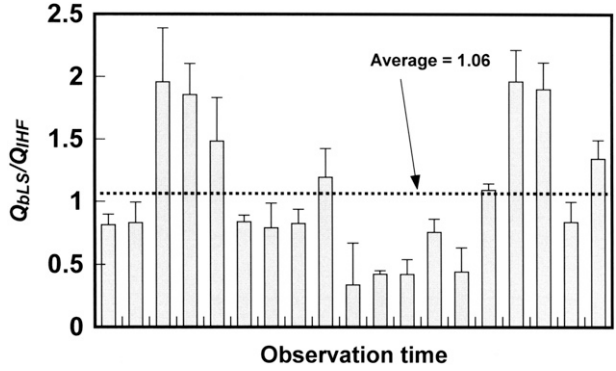


Fig. 22–6. Ratio of metolachlor emission rates from bLS and IHF measurements ($Q_{bLS}/Q_{IHF}$) for a series of 2- and 4- h periods. The observations span 5 d and are presented in chronological order (but not continuous). Error bars are the standard deviation of five simultaneous bLS estimates using $C$ taken at five measurement heights.

This is a much larger scale problem than the previous example, for here the field dimensions are hundreds of meters. This means that other micrometeorological techniques, such as flux-gradient methods, could be used to determine $Q$. In this case, however, the choice of the bLS technique might be still be attractive because of the *simplicity* of the needed field measurements.

## Ammonia Emissions from a Hog Waste Lagoon

Dzikowski et al. (1999) estimated ammonia emissions from a hog waste lagoon using the bLS technique. The lagoon was approximately 2800 $m^2$ in size and was surrounded by a low grass-covered berm (Fig. 22–7). The lagoon surface was approximately 1 m below the top of the berm, which gently fell away to the surrounding stubble field (1 to 2 m below the berm top). An open-path laser sensor was used to measure line-average ammonia concentration ($C_L$) across the lagoon, 1.4 m above the liquid surface.

Windspeed and temperature profiles were measured on the low berm to determine $S$, $z_0$, $L$, and $\beta$ (from a wind-vane). Lagoon emissions were estimated during a 52-h period, broken into 30-min intervals. Touchdown catalogs corresponding to the proper $L$ for each interval were rotated to the proper $\beta$ and translated to equi-spaced measurement points along the laser path. The example touchdown catalog in Fig. 22–7, which is for stable atmospheric stratification, is visually different from the unstable catalog in Fig. 22–5. Because of the lower turbulence in this stable atmosphere, the catalog is much narrower in the cross-wind direction (as can be deduced by inspection of the touchdown cloud where it spreads away from the ends of the line sensor) and the nearest touchdown points are seen to be much further from the sensor (reduced mixing means that source material passing through the sensor must come from a larger distance upwind).

North or easterly winds put the lagoon downwind of the barns and fence, which would presumably "disturb" the winds over the lagoon, and invalidate a MOST wind description. Wind from those directions also would bring ammonia from the hog barns over the lagoon, violating the assumption of a single ammonia source. Therefore, only periods with $\beta$ from 135 to 315° were used to calculate $Q_{bLS}$ (the aerodynamic effect of obstacles does not propagate very far upwind). Such selectiveness is recommended at complex sites[4]. Only 34% of measurement periods had wind directions that allowed "good" $Q_{bLS}$ estimates (Fig. 22–8). Dzikowski et al. (1999) then used other information to fill-in the missing gaps.

How accurate were the predictions? A mass balance technique based on the IHF (McGinn & Janzen, 1998) was used to independently estimate emissions ($Q_{IHF}$), and there was a single period of overlap between the bLS and IHF estimates. A four-hour $Q_{IHF}$ measurement was compared with five half-hour $Q_{bLS}$ measurements over the same interval. Here the average $Q_{bLS}$ was 79% of $Q_{IHF}$. If $Q_{IHF}$ is reduced 10% to account for turbulent flux, then the bLS estimate was within 15% of the IHF estimate. This was surprisingly good agreement, considering the bLS and IHF estimates relied on two different approaches for measuring

[4]When faced with a complex site there are three possibilities: (i) either select periods where MOST is likely upheld; (ii) use *all* observations but accept larger uncertainties in $Q_{bLS}$; or (iii) use a more sophisticated dispersion model that incorporates the true windflow complexity.

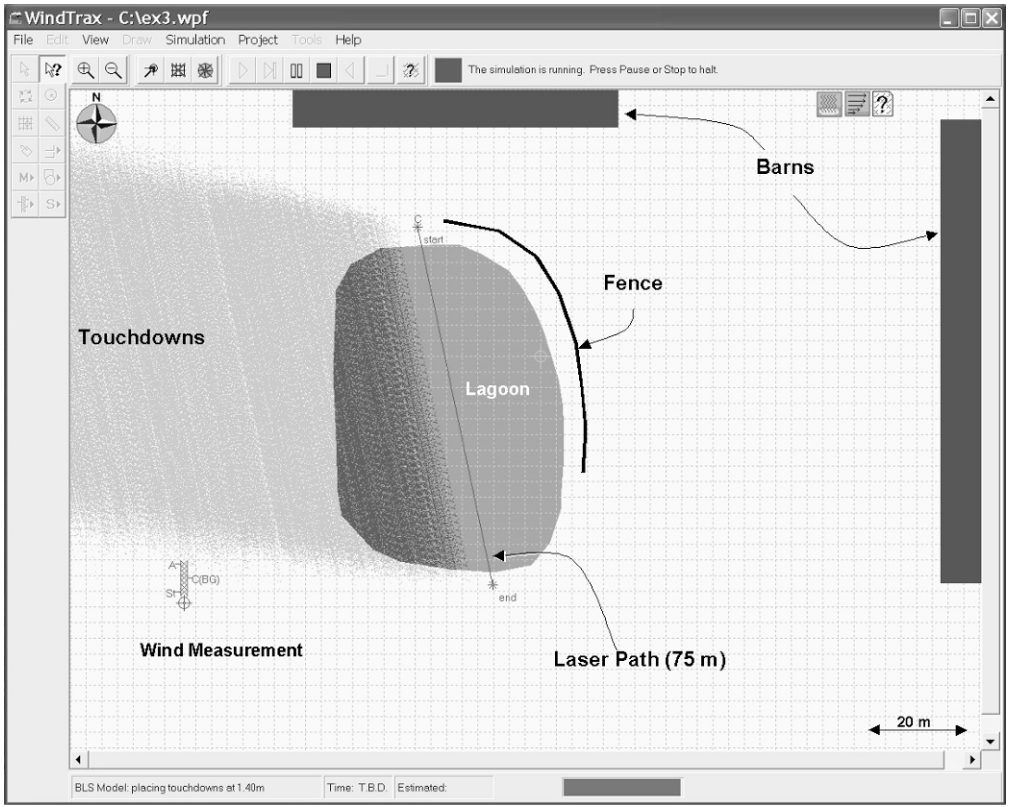


Fig. 22–7. Layout of the lagoon emission study. An open-path laser measured line-average concentration of ammonia across the lagoon. The small points to the left of the laser path are touchdowns for a measurement height $z_m$ = 1.4 m, a westerly wind ($\beta = 280°$), and a stable atmosphere ($L$ = 10 m).

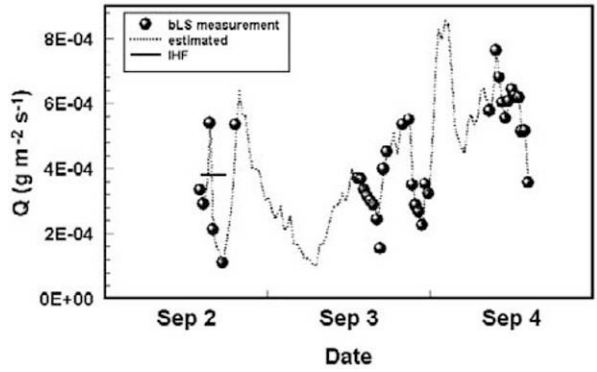


Fig. 22–8. Ammonia emission rates ($Q$) from the hog waste lagoon. The bLS estimates were made during suitable wind directions (barns downwind of the lagoon), and these data are indicated by circles. At other times $Q$ was estimated using a statistical model based on the surrounding $Q_{bLS}$ estimates. The short solid line on September 2 gives an IHF estimate of $Q$ during one 4-h period.

ammonia concentration (a salicylate technique versus an open-path laser), and the measurement footprints of the two estimates corresponded to different portions of the lagoon.

The sensitivity of the bLS estimates to measurement errors for this case is deduced from Table 22–1 (for westerly winds and neutral stability). For example, if the lagoon dimensions are increased by 10% while other parameters are unchanged, $Q_{bLS}$ will decrease by 22%. Here the bLS estimates are sensitive to errors in the mapping of source and sensor. Unlike the previous examples, the inferred $Q_{bLS}$ is sensitive to most measurement variables, including $z_0$, $L$, sensor location, and wind direction. Why the greater sensitivity? The $C_L$ observations in this case were nearer the upper edge of the tracer plume, a location where $(C_L/Q)_{sim}$ is very sensitive to atmospheric conditions and changes in the source location. A better choice would have been to decrease the laser height $z_m$ to 1.0 m, which would significantly reduce this sensitivity (Table 22–1).

This lagoon was not an ideal surface-layer site. The surrounding berm surely altered the wind and turbulence around the lagoon. The lagoon itself, a smooth liquid surface warmer or colder than the surrounding ground, would also act to modify the ambient aerodynamics. Yet from this short period of intercomparison, it would seem that the bLS technique does estimate emissions quite well. Apparently the departures from ideal MOST conditions were insignificant with regard to $Q_{bLS}$ predictions. This implies a robustness in MOST wind statistics despite topographic variations, and an insensitivity in tracer transport to disturbed surface aerodynamics.

## SUMMARY

The inverse-dispersion method overcomes some of the limits of traditional micrometeorological methods for estimating tracer emissions. It allows the determination of $Q$ without restrictions on the size and shape of the source, with less

onerous instrumentation requirements, and with considerable freedom in choosing convenient measurement locations. Furthermore the method can be easily adapted for use with line-average concentration sensors (i.e., open-path lasers), which not only are convenient but also provide for more accurate inference of emissions. The bLS technique described in this chapter is one implementation of the method. Besides the accuracy of the underlying bLS dispersion model, its advantage is the simplicity of application for ideal surface-layer problems (homogeneous sites where MOST accurately describes the windflow). Based on the examples given in this chapter, and on the results of other experiments (e.g., Denmead et al., 1998; McGinn & Jansen, 1997; Flesch et al., 2004), the technique is as accurate as other alternative methods.

The simplicity of the bLS technique depends on having a site where MOST is upheld. While more sophisticated dispersion models can be invoked for cases involving non-ideal settings, and $Q$ inferred for such problems, the simplicity of application is lost. Fortunately many agricultural and environmental problems meet the requirement that MOST give a reasonable picture of the winds, at least loosely. An important research question is how far can one move away from an ideal surface-layer problem, yet retain the accuracy of a simple bLS technique based on MOST? The theoretical study of Wilson et al. (2001) looked at this issue in a lagoon setting, where the aerodynamic environment evolves as the wind moves from the surrounding upwind land surface to a smoother and warmer–cooler lagoon surface. They found that bLS estimates of $Q$ from the lagoon, inferred with a MOST bLS model, were relatively insensitive to the aerodynamic modifications induced by the lagoon. This is encouraging, as it suggests robustness of the technique. And a preliminary field study by Flesch et al. (2005) found that even for a tracer source in a dramatically "disturbed" aerodynamic environment (a source surrounded by a fence), it was possible to use the simple bLS method to accurately infer emissions by avoiding measurement locations near the source of the wind disturbance (i.e., the fence).

The bLS technique is just one of many possible implementations of the inverse-dispersion method for inferring emissions. It has the advantage that, when applied to situations where MOST is upheld, or the departure from MOST is minimal, it is both easy to use and demonstrably accurate. Irrespective of the bLS technique, inverse-dispersion methods for calculating emissions will become increasingly important. The need to evaluate emissions from complex sites where traditional methods cannot be applied, along with the increasing capability of dispersion models and wind flow models, guarantees this will be the case.

## REFERENCES

Aylor, D.E., and T.K. Flesch. 2001. Estimating spore release rates using a Lagrangian stochastic simulation model. J. Appl. Meteorol. 40:1196–1208.

Carter, R.E., D.D. Lane, G.A. Marotz, C.T. Chaffin, T.L. Marshall, M. Tucker, M.R. Witkowski, R.M. Hammaker, W.G. Fateley, M.J. Thomas, and J.L. Hudson. 1993. A method of predicting point and path averaged ambient air VOC concentrations using meteorological data. J. Air Waste Manage. 43:480–488.

Denmead, O.T., L.A. Harper, J.R. Freney, D.W.T. Griffith, R. Leuning, and R.R. Sharpe. 1998. A mass balance method for non-intrusive measurements of surface-air trace gas exchange. Atmos. Environ. 32:3679–3688.

Denmead, O.T., and M.R. Raupach, 1993. Method for measuring atmospheric gas transport in agricultural and forest systems. p. 19–43. *In* Agricultural ecosystem effects on trace gases and global climate change. ASA Spec. Publ. 55. ASA, Madison, WI.

Dzikowski P, H. Bertram, T. Flesch, S. McGinn, A. Arendt, and T. Coates. 1999. Measuring ammonia emissions from liquid hog manure storage lagoons and land applications. Alberta Agric. Res. Inst. Rep. Alberta Res. Inst., Edmonton.

Flesch, T.K., J.H. Prueger, and J.L. Hatfield. 2002. Turbulent Schmidt number from a tracer experiment. J. Agric. For. Meteorol. 111:299–307.

Flesch, T.K., J.D. Wilson, and L.A. Harper. 2005. Deducing ground-to-air emissions from observed trace gas concentrations: A field trial with wind disturbance. J. Appl. Meteorol. In press.

Flesch, T.K., J.D. Wilson, L.A. Harper, B.P. Crenna, and R.R. Sharpe. 2004. Deducing ground-to-air emissions from observed trace gas concentrations: A field trial. J. Appl. Meteorol. 43:487–502.

Flesch, T.K., J.D. Wilson, and E. Yee. 1995. Backward-time Lagrangian stochastic dispersion models, and their application to estimate gaseous emissions. J. Appl. Meteorol. 34:1320–1332.

Garratt, J.R., 1992. The atmospheric boundary layer. Cambridge Univ. Press, New York.

Gifford, F.A. 1976. Turbulent diffusion typing schemes: A review. Nucl. Safety 17:68–85.

Hanna, S.R. 1982. Applications in air pollution modelling. p. 275–310. *In* F.T.M. Nieuwstadt and H. van Dop (ed.) Atmospheric Turbulence and air pollution modelling. Reidel Publishing, Boston.

McGinn, SM, and H.H. Janzen. 1998. Ammonia sources in agriculture and their measurement. Can. J. Soil Sci.78:139–148.

Panofsky, H.A., H. Tennekes, D.H. Lenschow, and J.C. Wyngaard. 1977. The characteristics of turbulent velocity components in the surface layer under convective conditions. Bound.-Layer Meteorol. 11:355–361.

Pasquill, F. 1961. The estimation of the dispersion of windborne material. Met. Mag. 90:33–49.

Raupach, M.R. 1989. A practical Lagrangian method for relating scalar concentrations to source distributions in vegetative canopies. Quart. J.R. Meteorol. Soc. 115:609–632.

Rodean, H.C. 1996. Stochastic lagrangian models of turbulent diffusion. Meteorological Monogr. no. 48. Am. Meteorol. Soc., Boston.

Seibert, P. 1999. Inverse modelling of sulfur emissions in Europe based on trajectories. p. 147–154. *In* Prasad Kasibhatla et al. (ed.) Inverse methods in global biogeochemical cycles. AGU Geophysical Monogr. Series. Vol. 114. Am. Geophys. Union, Washington, DC.

Thomson, D.J. 1987. Criteria for the selection of stochastic models of particle trajectories in turbulent flows. J. Fluid Mech. 180:529–556.

Wilson J.D., T.K. Flesch, and L.A. Harper. 2001. Micrometeorological methods for estimating surface exchange with a disturbed windflow. J. Agric. For. Meteorol. 107:207–225.

Wilson, J.D., and B.L. Sawford. 1996. Review of Lagrangian stochastic models for trajectories in the turbulent atmosphere. Bound-layer Meteorol. 78:191–210.

Wilson, J.D., and W.K.N. Shum. 1992. A re-examination of the integrated horizontal flux method for estimating volatilisation from circular plots. Agric. For. Meteorol. 57:281–295.

Wilson, J.D., G.W. Thurtell, and G.E. Kidd. 1981. Numerical simulation of particle trajectories in inhomogeneous turbulence: III. Comparison of predictions with experimental data for the atmospheric surface-layer. Bound.-Layer Meteorol. 21:443–463.

Wilson, J.D., G.W. Thurtell, G.E. Kidd, and E.G. Beauchamp. 1982. Estimation of the rate of gaseous mass transfer from a surface source plot to the atmosphere. Atmos. Environ. 16:1861–1867.